J|A|C|S
COMMUNICATIONS

Published on Web 01/26/2007

Framework-Catenation Isomerism in Metal−Organic Frameworks and Its Impact on Hydrogen Uptake

Shengqian Ma,[†] Daofeng Sun,[†] Michael Ambrogio,[†] Jacqueline A. Fillinger,[†] Sean Parkin,[‡] and Hong-Cai Zhou*,[†]

Department of Chemistry & Biochemistry, Miami University, Oxford, Ohio 45056, and Department of Chemistry, University of Kentucky, Lexington, Kentucky 40506

Received October 17, 2006; E-mail: zhouh@muohio.edu

Recent studies have focused on metal−organic frameworks (MOFs) with high hydrogen uptake[1] in order to reach the 2010 DOE targets for on-board vehicular hydrogen storage.[2] Strategies such as using pore sizes comparable to hydrogen molecules[3] and introducing coordinatively unsaturated metal centers (UMCs)[3b,c,4] have been explored. Recently, we have reported a biomimetic approach to UMCs utilizing entatic metal centers (EMCs).[5] We have also demonstrated in both PCN-6[3c] (porous coordination networks) and PCN-9[5] that interpenetration is an important factor contributing to their respective hydrogen uptake. However, interpenetration (or framework catenation) as an *independent* criterion has never been resolved from other factors. Normally in a given metal−ligand combination, *either* an interpenetrated network *or* a non-interpenetrated network is favored, not both. Conceptually, an interpenetrated MOF and its non-interpenetrated counterpart can be viewed as a supramolecular pair of stereoisomers. In reality, however, such *framework-catenation isomerism* has never been deliberately explored prior to the present report. To study the precise role of catenation in hydrogen uptake, using oxalate as a template, we have made the non-interpenetrated counterpart of PCN-6 (PCN-6′).

At solvothermal conditions, a reaction between $Cu(NO_3)_2 \cdot 2.5H_2O$ and H_3TATB in the presence of oxalic acid afforded turquoise octahedral crystals of PCN-6′ (yield: 60%). TATB represents 4,4′,4″-*s*-triazine-2,4,6-triyl-tribenzoate. The reaction was run in dimethylacetamide (DMA) at 75 °C. The overall formula of PCN-6′ is $Cu_6(H_2O)_6(TATB)_4 \cdot DMA \cdot 12H_2O$, determined by X-ray crystallography, elemental analysis, and thermogravimetric analysis (TGA).

Singe-crystal X-ray[6] diffraction studies reveal that PCN-6′ crystallizes in cubic space group *Fm*-3*m*. It is isostructural with HKUST-1,[7] mesoMOF-1,[8] and with a single net of the interpenetrated PCN-6.[3c] In PCN-6′, dicopper tetracarboxylate paddlewheel SBUs (secondary building units) are linked by TATB bridges. Each SBU connects four TATB ligands, and each TATB binds three SBUs to form a T_d-octahedron (Figure 1b), which has idealized T_d symmetry with four ligands covering alternating triangular faces of the octahedron and an SBU occupying each vertex. Eight such T_d-octahedra occupy the eight vertices of a cube to form a cuboctahedron through corner sharing with idealized O_h symmetry (Figure 1a).[3c] The average diameter of the void inside the cuboctahedron is 30.32 Å. Every cuboctahedron connects eight T_d-octahedra via face-sharing, and each T_d-octahedron links four cuboctahedra to form a three-dimensional framework with a twisted boracite net topology (Figure 1c). Open square channels from all three orthogonal directions are identical in size and are 15.16 × 15.16 Å^2 or 21.44 × 21.44 Å^2 along the edges or diagonals,

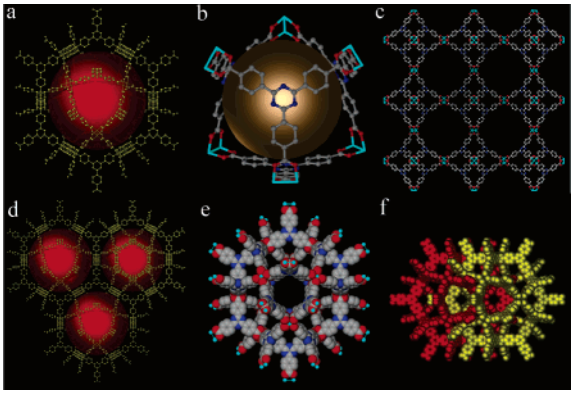

Figure 1. (a) Cuboctahedral cage; (b) *Td*-octahedral cage; (c) a view of the packing of PCN-6′ from the [001] direction; (d) a view of the cuboctahedral net from the [111] direction of PCN-6′; (e) space-filling model of the non-interpenetrated net in PCN-6′; (f) two interpenetrated nets in PCN-6. The large spheres shown in graphics a, b, and d represent void inside the cages.

respectively (atom to atom distance). Alternatively the structure can be described as four honeycomb nets connected by the SBUs at the center of the hexagonal-edges; the TATB ligands occupy the corners of each hexagon and each hexagon is in a chair conformation (Figure 1d).

The structure of PCN-6 (space group *R*-3*m*) can be reproduced by two identical interpenetrated nets of PCN-6′, the second being generated by translation of the first by *c*/5 (*c* represents the *c*-axis in PCN-6) along [111] direction of PCN-6′. PCN-6′ and PCN-6 are thus catenation isomers (Figure 1e,f). To the best of our knowledge, this is among the first pairs of such catenation isomers.[3b]

Variables in the synthetic procedures of PCN-6 and PCN-6′ include temperature, solvent, and template addition. Controlled experiments were performed to confirm that template addition is the only factor determining the final topology. Without the addition of oxalic acid, the reaction between $Cu(NO_3)_2 \cdot 2.5H_2O$ and H_3TATB in DMA, dimethylformamide (DMF), or diethylformamide (DEF) at 75 °C or 120 °C (with DMSO as solvent) led to the formation of PCN-6. In contrast, with oxalic-acid addition the same reaction in DMA, DMF, or DEF at 75 °C or 120 °C (DMSO) gives PCN-6′. Thus, only template addition can account for the presence or absence of catenation.

To test the general pertinence of this finding, another large trigonal-planar ligand HTB (for *s*-heptazine tribenzoate)[9] was employed to react with $Cu(NO_3)_2 \cdot 2.5H_2O$ under reaction conditions similar to those of PCN-6 and PCN-6′. As expected, an interpenetrated MOF isostructural with PCN-6 (MOF−HTB) was obtained without the addition of oxalic acid, while a non-interpenetrated MOF isostructural with PCN-6′ (MOF−HTB′) was

[†] Miami University.
[‡] University of Kentucky.

10.1021/ja067435s CCC: $37.00

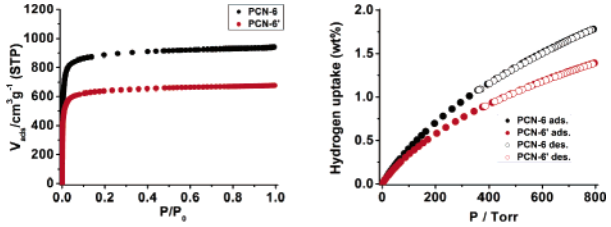

Figure 2. Gas sorption isotherms (77 K) of PCN-6′ and PCN-6 activated at 50 °C for N_2 (left) and H_2 (right).

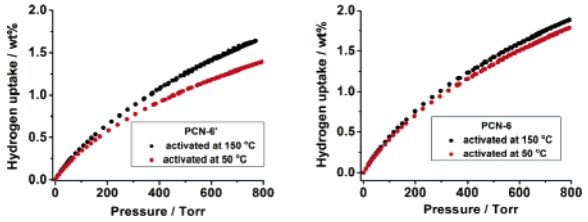

Figure 3. H_2 sorption isotherms of PCN-6′ (left) and PCN-6 (right) activated at 50 and 150 °C.

formed in the presence of oxalic acid. The mechanistic details of this remarkable templating effect are still under investigation.

Both PCN-6′ and PCN-6 exhibit permanent porosity, confirmed by gas sorption (Figure 2) and powder X-ray diffraction (PXRD) studies (Figure S5). In contrast, both HTB MOFs collapse upon guest solvent removal presumably owing to the instability of the larger open channels in the two HTB MOFs. The N_2 adsorption isotherm of PCN-6′ (Figure 2a) indicates typical Type-I sorption behavior, with a Langmuir surface area of 2700 m^2/g (pore volume 1.045 mL/g). This is lower than the Langmuir surface area of PCN-6 (3800 m^2/g, pore volume 1.453 mL/g), although PCN-6′ has a higher solvent-accessible volume (86%, calculated using PLATON[10]) than that of PCN-6 (74%). Thus, catenation has led to 41% increase in Langmuir surface area. This counter-intuitive increase can be attributed to that the new adsorption sites are formed by the catenation as well as the small pores formed as a result of catenation may strengthen the overall interaction between gas molecules and the pore walls therefore increase the *apparent* surface area, as predicted by a recent theoretical simulation.[11] If open channels are blocked as a result of catenation, however, the overall surface area may drop significantly.

It is important to study the independent contribution of catenation to hydrogen uptake. In the catenation isomer pair of PCN-6 and PCN-6′, the contributions from interpenetration and UMCs must be separated. TGA studies on the two MOFs suggest that activation at 50 °C will remove only guest molecules. To expose the UMCs, the samples must be heated at 150 °C to remove the axial aqua ligands on the Cu centers. A facile way to resolve the contributions by UMCs and catenation to hydrogen uptake is to measure the hydrogen adsorption isotherms of samples activated at the two temperatures.

Hydrogen adsorption studies revealed that PCN-6′ activated at 50 °C can adsorb 1.35 wt % (volumetric uptake of 3.94 kg/m^3, calculated density: 0.292 g/cm^3) hydrogen at 760 Torr and 77 K (Figure 2b), significantly lower than that of PCN-6 activated at the same temperature (1.74 wt %; volumetric uptake of 9.19 kg/m^3, calculated density: 0.528 g/cm^3). Hence, catenation has led to a 133% of enhancement in volumetric (29% in gravimetric) hydrogen uptake. Previously we have reported that after activation at 150 °C, PCN-6 can adsorb 1.9 wt % hydrogen (at 760 Torr and 77 K), a 10% improvement over that of PCN-6 activated at 50 °C (Figure 3). Similarly, after activation at 150 °C, PCN-6′ can adsorb 1.62 wt % hydrogen, a 20% increase from that of PCN-6′ activated at 50 °C (Figure 3). These further improvements upon activation at 150 °C can only be attributed to UMCs. The smaller improvement of hydrogen uptake upon UMC activation in PCN-6 than that in PCN-6′ suggests that most of the UMCs in PCN-6 are blocked as a result of catenation (observed from the crystal structure), while the UMCs in PCN-6′ are open.

In summary, using an unprecedented templating strategy, new catenation isomer-pairs can be synthesized predictably using copper paddlewheel SBUs and two trigonal-planar ligands (TATB and HTB) developed in our lab. Gas sorption studies on the isomer pair using TATB have revealed that catenation leads to a 41% improvement of Langmuir surface area and a 133% increase in volumetric hydrogen uptake (29% increase in gravimetric). The resolution of the contributions from UMCs and catenation to the hydrogen uptake of a MOF is unprecedented. Future work will focus on investigating the mechanistic details of oxalate-templating and applying this strategy to other systems.

Acknowledgment. This work was supported by the National Science Foundation (Grant CHE-0449634) and Miami University. H.C.Z. also acknowledges the Research Corporation for a Research Innovation Award and a Cottrell Scholar Award. The diffractometer was funded by NSF Grant CHE-0319176 (S.P.).

Supporting Information Available: Detailed experimental procedures, X-ray structural data (cif files), PXRD patterns, TGA graphics. This material is available free of charge via the Internet at http://pubs.acs.org.

References

(1) (a) Rowsell, J. L. C.; Millward, A. R.; Park, K. S.; Yaghi, O. M. *J. Am. Chem. Soc.* **2004**, *126*, 5666. (b) Rowsell, J. L. C.; Eckart, J.; Yaghi, O. M. *J. Am. Chem. Soc.* **2005**, *127*, 14904. (c) Kesanli, B.; Cui, Y.; Smith Milton, R.; Bittner Edward, W.; Bockrath Bradley, C.; Lin, W. *Angew. Chem., Int. Ed.* **2005**, *44*, 72. (d) Lee, J. Y.; Pan, L.; Kelly, S. P.; Jagiello, J.; Emge, T. J.; Li, J. *Adv. Mater.* **2005**, *17*, 2703. (e) Sun, D.; Ke, Y.; Mattox, T. M.; Betty, A. O.; Zhou, H.-C. *Chem. Commun.* **2005**, 5447. (f) Panella, B.; Hirscher, M. *Adv. Mater.* **2005**, *17*, 538. (g) Rowsell, J. L. C.; Yaghi, O. M. *J. Am. Chem. Soc.* **2006**, *128*, 1304. (h) Wong-Foy, A. G.; Matzger, A. J.; Yaghi, O. M. *J. Am. Chem. Soc.* **2006**, *128*, 3494. (i) Chen, B.; Ma, S.; Zapata, F.; Lobkovsky, E. B.; Yang, J. *Inorg. Chem.* **2006**, *45*, 5718. (j) Dincă, M.; Yu, A. F.; Long, J. R. *J. Am. Chem. Soc.* **2006**, *128*, 8091. (k) Li, Y.; Yang, R. T. *J. Am. Chem. Soc.* **2006**, *128*, 726. (l) Li, Y.; Yang, R. T. *J. Am. Chem. Soc.* **2006**, *128*, 8136.
(2) (a) Schlapbach, L.; Zuttel, A. *Nature* **2001**, *414*, 353. (b) Hydrogen, Fuel Cells & Infrastructure Technologies Program: Multi-year Research, Development, and Demonstration Plan. U.S. Dept. of Energy, 2005, http://www.eere.energy.gov/hydrogenandfuelcells/mypp/.
(3) (a) Pan, L.; Sander, M. B.; Huang, X.; Li, J.; Smith, M. R., Jr.; Bittner, E. W.; Bockrath, B. C.; Johnson, J. K. *J. Am. Chem. Soc.* **2004**, *126*, 1308. (b) Rowsell, J. L. C.; Yaghi, O. M. *Angew. Chem., Int. Ed.* **2005**, *44*, 4670 and references therein. (c) Sun, D.; Ma, S.; Ke, Y.; Collins, D. J.; Zhou, H.-C. *J. Am. Chem. Soc.* **2006**, *128*, 3896.
(4) (a) Chen, B. L.; Ockwig, N. W.; Millward, A. R.; Contreteas, D. S.; Yaghi, O. M. *Angew. Chem., Int. Ed.* **2005**, *44*, 4745. (b) Dietzel, P. D. C.; Panella, B.; Hirscher, M.; Blom, R.; Fjellvag, H. *Chem. Commnun.* **2006**, 959. (c) Yang, Q.; Zhong, C. *J. Phys. Chem. B* **2006**, *110*, 655.
(5) Ma, S.; Zhou, H.-C. *J. Am. Chem. Soc.* **2006**, *128*, 11734.
(6) X-ray crystal data for PCN-6′: $C_{32}H_{16}Cu_2N_4O_{10}$, fw = 743.59, cubic, *Fm*-3*m*, a = 46.636(5) Å, b = 46.636(5) Å, c = 46.636(5) Å, V = 101432-(20) Å^3, Z = 24, T = 250 K, ρ_{calcd} = 0.292 g/cm^3, R_1 ($I > 2\sigma(I)$) = 0.0650, wR_2 (all data) = 0.1605.
(7) Chui, S. S.-Y.; Lo, S. M.-F.; Charmant, J. P. H.; Orpen, A. G.; Williams, I. D. *Science* **1999**, *283*, 1148.
(8) Wang, X.-S.; Ma, S.; Sun, D.; Parkin, S.; Zhou, H.-C. *J. Am. Chem. Soc.* **2006**, *128*, 16474.
(9) Ke, Y.; Collins, D. J.; Sun, D.; Zhou, H.-C. *Inorg. Chem.* **2006**, *45*, 1897.
(10) Spek, A. L. *J. Appl. Crystallogr.* **2003**, *36*, 7.
(11) Jung, D. H.; Kim, D.; Lee, T. B.; Choi, S. B.; Yoon, J. H.; Kim, J.; Choi, K.; Choi, S.-H. *J. Phys. Chem. B* **2006**, *110*, 22987.

JA067435S